

On Theoretical Accuracy of Meteorological Targets Measurement by Radar

Ondrej FISER¹, Maria KOVALCHUK^{1,2}

¹ Faculty of Electrical Engineering and Informatics, University of Pardubice,
nám. Čs. legií 565, 532 10 Pardubice, Czech Republic

² Institute of Atmospheric Physics AS CR, Boční II 1401/1A, 141 00 Praha 4, Czech Republic

ondrej.fiser@upce.cz, maria.kovalchuk@ufa.cas.cz

Submitted September 6, 2021 / Accepted March 21, 2022

Abstract. *We draw your attention to the fact that meteorological radar does not actually measure a commonly used quantity “radar reflectivity factor,” (which is not dependent on frequency) but a different quantity called “radar reflectivity.” We present the usual recalculation which is based on frequency dependency used by Rayleigh approximation of radar cross-sections (back scattering cross section of rain, cloud, fog drop). But this approximation is valid in Rayleigh region only. We concluded that for admitting error lower than 2 dB in the radar reflectivity factor determination we can use the “effective radar reflectivity factor” for frequencies up to 19 GHz only. Otherwise the error will increase. As we use (and present in this article) the Mie algorithm we can replace the Rayleigh frequency dependence estimation by more accurate radar reflectivity factor determination using the Mie scattering. The correction is presented in the form of “Correction function C” dependent on frequency and rain rate in the graphical form and polynomial approximation. Beside this we present the simplification of back scattering cross sections for Rayleigh and Optical regions and the border values of size parameter for these regions. We added the meteorological radar equation derivation. This should support the radar measurement understanding.*

Keywords

Electromagnetic reflection, meteorological radar, radar cross-sections, radar measurements

1. Introduction

Meteorological radars play a big role in meteorology, weather and hazardous situation prediction, monitoring of large weather systems etc. It helps to understand physics of atmosphere and last but not least radars support the radio-wave propagation condition research.

From beginning, the meteorological radars were constructed for S band (2–4 GHz) and later for C band (4–8 GHz) and methods of data processing were prepared

for these bands. For instance, the European meteorological radar network “OPERA” operates C band radars [1]. But now meteorological radars work also at higher frequencies: X-band (8–12.5 GHz), Ka band (26.5–40 GHz) and especially for cloud and melting layer observation [2], [3] also at W (94 GHz) and G bands (110–300 GHz). “Old” methods suggested for S and C bands are not accurate as we show in this study. It means that it is necessary to find functions, which can compensate deviations in computation and data processing for higher frequencies. Thus for the right weather radar utilization in propagation and meteorology, correct radar data processing and understanding are needed.

One of problems is that the radar measurement is dependent on used frequency and therefore a physical quantity “radar reflectivity factor” (not dependent on frequency) was defined (26), (27) and is broadly used especially in meteorology and in radiowave propagation research. This quantity is not directly measured but is computed from the measured radar reflectivity supposing the Rayleigh approximation of the back scattering cross sections of meteorological targets. More precisely: the replacement of the radar reflectivity factor is performed by the equivalent radar reflectivity factor based on the estimation of frequency dependence which is used in the Rayleigh approximation. But this frequency dependence causes not negligible error growing with frequency. This is described in details in next sections. A mention of this problem is also in [4] in the form of a brief note.

Other motivation to write this article was to specify the Rayleigh and optical regions for the back scattering cross-section calculations of meteorological targets accurately. We found the borders for these regions (instead of uncertain, but well known conditions $x \ll 1$ or $x \gg 1$, where x is size parameter (for its definition see equation (18) and below) and published here the simple substitutions. In next section we briefly introduce the radar equation derivation in the case of meteorological radars, for more see [5], [6].

The existence of more complex radars (two-wave, three-wave, Doppler) is worth mentioning. In [3], for example, the advantages of double-wave radars using cer-

tain frequency pairs, such as Ka-G pair, are explained. This pair is also suitable for the DWR (Dual Wavelength Ratio) determination which is by 4 dB more significant than in the traditional Ka-W band pair. This allows the detection of small atmospheric particles. Study in [3] also describes the advantages of the individual frequency bands used by meteorological radars, e.g. G band radars can detect melting layer. Doppler two-wave radars operating for example in Ka-W bands can also determine DSD (Drop Size Distribution) [7].

The radar research of atmospheric turbulences concerning also the Bragg scattering is shown in [4]. Here, it is also shown how to estimate the useful quantity “refractive index structure constant $C_n^{2\prime\prime}$ ” from the measured radar reflectivity. Study [4] shows also a simple model of the frequency scaling of the equivalent radar reflectivity factor.

DWR was already used as a parameter of atmospheric research in the 1950s, when the “dB” difference between radar reflectivity factor at 9.5 and 2.9 GHz was reported. It was called “hail signal” serving for hail detection.

Other important class of meteorological radar is working with polarimetry [6]. Its outputs ZDR (differential reflectivity), LDR (Linear Depolarization Ratio), CDR (Circular Depolarization Ratio), Φ DP (Differential Phase Shift) and KDP (Specific Differential Phase) support the atmospheric particle identification, measurement accuracy etc.

2. Radar Equation in Meteorology

The classical radar equation for the monostatic radar and one target is as follows:

$$P_r = \frac{\lambda^2 \cdot G^2 \cdot P_t}{(4\pi)^3} \cdot \frac{\sigma}{r^4} = K_r \cdot \frac{\sigma}{r^4} \quad [\text{W}] \quad (1)$$

where P_r (P_t) is the received (transmitted) radar power, λ is the wave length [m], G is the radar antenna gain [-], σ is the effective back scattering cross section of the target [m^2], r is the radar-target distance [m], K_r is the radar constant [Wm^{-2}].

If there are many particular targets (rain drops, fog or cloud droplets etc.) the effective back scattering cross sections of particular targets (drops) must be summed. We express it through the quantity “radar reflectivity η ,” which is defined per unit volume [5]:

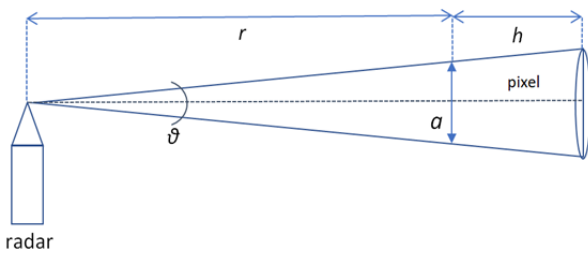


Fig. 1. On pixel (radar volume) computation.

$$\eta = \frac{\sum \sigma(D)}{V} \quad [\text{mm}^2\text{m}^{-3}] \quad (2)$$

where D is the equivolumetric rain drop or cloud (fog) droplet diameter, V is the radar volume (pixel, bin), see (5).

If the drop size distribution (DSD) of the target is known (see [8], for instance), the expression for the radar reflectivity could be also written as:

$$\eta = \int_0^\infty \sigma(D) \cdot N(D) \cdot dD \quad [\text{mm}^2\text{m}^{-3}] \quad (3)$$

where D is the equivolumetric drop diameter ($D = 2a$, a is equivolumetric drop radius), $N(D)$ is the drop size distribution (DSD) defined as the number of drops of the diameter between D and $D + dD$ per unit volume. For DSD examples see [8], [9] and (31).

It is easy to derive the radar volume V (see Fig. 1). The area S of the pixel base is:

$$S = \frac{\pi \vartheta^2 r^2}{4} \quad [\text{m}^2] \quad (4)$$

where r is the radar–target distance, ϑ is the antenna beam width in radians.

The radar volume V can be obtained from [6], i.e.

$$V = S \cdot h \cdot \frac{1}{2 \ln 2} \quad [\text{m}^3] \quad (5)$$

where h is the radar pixel length; in the case of pulse radars it is

$$h = \frac{c \cdot \tau}{2} \quad [\text{m}] \quad (6)$$

where c is the light speed and τ is the pulse lengths.

The value $1/(2 \ln 2) \sim 0.72$ comes from the nonuniform distribution of energy in the radar cone beam when the Gaussian distribution is supposed, see [6].

The radar equation in meteorology is then logically expressed as follows:

$$P_r = \frac{\lambda^2 \cdot G^2 \cdot P_t \cdot \vartheta^2 \cdot c \cdot \tau}{2^{10} \cdot \pi \cdot \ln 2} \cdot \frac{\eta}{r^2} = C_r \cdot \frac{\eta}{r^2} \quad [\text{W}] \quad (7)$$

where ϑ is the 3dB beam width [rad], C_r is the radar constant in the meteorological radar case [$\text{W m}^5 \text{mm}^{-2}$]. This equation is called Probert-Jones Radar Equation.

Through (7) the radar measures the radar reflectivity η . In fact, it is the average radar reflectivity in the whole radar volume V .

3. Back Scattering Functions after Mie

Mie scattering is limited on homogenous spheres and is valid for any value of size parameter x . To determine the scattering of an electromagnetic wave from isolated target

(raindrop etc.), the complex scattering functions \hat{f} (or \hat{S}) for different polarizations are used (for instance \hat{S}_h is the scattering function for horizontal polarization). The target cross sections can be computed also from scattering functions.

Scattering function \hat{S} can be, for instance, defined as follows [10]:

$$\hat{E}^s = \hat{E}^i \cdot \hat{S}(\mathbf{K}_1, \mathbf{K}_2) \cdot (jk_0z)^{-1} \cdot \exp(-jk_0z) \quad (8)$$

where \hat{E}^s is a phasor of scattered electric field intensity [V/m], \hat{E}^i is the phasor of the intensity of the incident electric field [V/m], $\hat{S}(\mathbf{K}_1, \mathbf{K}_2)$ is the complex scattering (dimensionless) function of the drop for the direction of incident wave \mathbf{K}_1 and the direction of scattered wave \mathbf{K}_2 , z is the distance of the scattered electric field intensity from the center of the drop, k_0 is the vacuum wave number [m⁻¹].

There is also another but similar definition of scattering function \hat{f} [11]:

$$\hat{E}^s = \hat{E}^i \cdot \hat{f}(\mathbf{K}_1, \mathbf{K}_2) \cdot (z)^{-1} \cdot \exp(jk_0z) \quad (9)$$

where $\hat{f}(\mathbf{K}_1, \mathbf{K}_2)$ is the complex scattering function of the drop ([m], usual dimension is also [cm]) for the direction of incident \mathbf{K}_1 and scattered waves \mathbf{K}_2 .

Special cases:

- a) if $\mathbf{K}_1 = \mathbf{K}_2$, it is the forward scattering;
- b) if $\mathbf{K}_1 = -\mathbf{K}_2$, it sounds for the backward scattering (important for radars);
- c) other cases of $\mathbf{K}_1, \mathbf{K}_2$. mutual orientations indicates the bi-static scattering.

For many studies the simplified spherical model of actual rain drop shape is permissible and only this one is used in our study. It enables to study the frequency and temperature dependence, however the polarization and depolarization cannot be investigated.

In [12], we have published a simple generator of forward scattering functions for spherical scattering drops. Based on it we present here similar algorithmic numerical generator of backward scattering functions \hat{S} based on Mie scattering theory [13, 14, 15]:

Starting values:

$$\hat{y} = \hat{m}x,$$

\hat{m} is the complex refractive index of rain drop water [24], [25],

x is size parameter (for definition see (18) and below),

$$\hat{A}_0 = \cotg \hat{y},$$

$$\hat{O}_0 = \sin x + j \cos x,$$

$$\hat{O}_{-1} = \cos x - j \sin x.$$

Mie series for scattering functions \hat{S} (8) on spherical targets:

$$\hat{S} = \sum_{n=1}^{N_{\max}} (-1)^{n+1} (2n+1) (\hat{a}_n - \hat{b}_n) \quad (10)$$

where

$$\hat{a}_n = \frac{\left[\frac{\hat{A}_n + \frac{n}{x}}{\hat{m}} \right] \text{Re} \hat{O}_n - \text{Re} \hat{O}_{n-1}}{\left[\frac{\hat{A}_0 + \frac{n}{x}}{\hat{m}} \right] \hat{O}_n - \hat{O}_{n-1}}, \quad (11)$$

$$\hat{b}_n = \frac{\left[\frac{\hat{m} \hat{A}_0 + \frac{n}{x}}{\hat{m}} \right] \text{Re} \hat{O}_n - \text{Re} \hat{O}_{n-1}}{\left[\frac{\hat{m} \hat{A}_n + \frac{n}{x}}{\hat{m}} \right] \hat{O}_n - \hat{O}_{n-1}}, \quad (12)$$

$$\hat{A}_n = -\frac{n}{\hat{y}} + \left[\frac{n}{\hat{y}} - \hat{A}_{n-1} \right]^{-1}, \quad (13)$$

$$\hat{O}_n = \frac{2n-1}{x} \hat{O}_{n-1} - \hat{O}_{n-2}. \quad (14)$$

Theoretically, N_{\max} should be infinity (i.e. very large number). But in such case some numerical problems during computer evaluation can occur so N_{\max} must be carefully estimated. For N_{\max} next recommendation is usually used [29]:

$$N_{\max} = x + 4x^{1/3} + 1 \quad \text{for } 0.02 < x < 8,$$

$$\text{for } N_{\max} \text{ it holds then } 2 < N_{\max} < 17,$$

$$N_{\max} = x + 4.05 x^{1/3} + 2 \quad \text{for } 8 < x < 4\,200,$$

$$\text{for } N_{\max} \text{ it holds then } 18 < N_{\max} < 4\,267,$$

$$N_{\max} = x + 4x^{1/3} + 2 \quad \text{for } 4200 < x < 20000,$$

$$\text{for } N_{\max} \text{ it holds then } 4267 < N_{\max} < 20111.$$

Scattering function \hat{f} can be derived from \hat{S} through equations (8) and (9):

$$\hat{f} = -j \frac{\lambda}{2\pi} \cdot \hat{S}^*.$$

Software for Mie scattering is also available in [15]. Experiments measuring the Mie and Rayleigh scattering are described, for instance, in [16].

Cloud, fog droplets and very small rain drops are of the spherical shape. It is not true for medium and big rain drops of diameter above 1 mm while the physical maximum of rain drop diameter is 7 mm. The actual rain drop shape [17] is shown in Fig. 2.

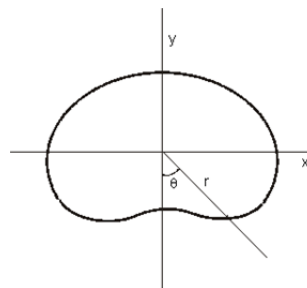


Fig. 2. The actual rain drop shape.

For non-spherical raindrops, the calculation of scattering functions is more difficult and is performed numerically. The results are then tabulated. Extended methods for scattering functions calculation are based on the Fredholm integral equation method, perturbation methods, MMP (multiple multi-pole) methods, point-matching method, DDA (Discrete Dipole Approximation) and others. The mentioned algorithms and results were published in the 1970s and 1980s by Dr. Tomohiro Oguchi [18], [19], Dr. Hajny [20], Dr. Mario Maggiori [21], Dr. Uzunoglu [11] and others. DDA method is also offered in the form of software packages, which is described in [22] also with more classical methods. Also [23] is devoted to scattering on hydrometeors.

4. Back Scattering Cross Section (RCS) of Meteorological Targets and its Computation

Definition of back scattering cross section of any isolated target is as follows:

$$\sigma \approx \frac{\text{scattered energy towards the source / unit angle}}{\text{density of incident energy / } 4\pi} \tag{15}$$

$$= \lim_{R \rightarrow \infty} 4\pi R^2 \left| \frac{\mathbf{E}_s}{\mathbf{E}_i} \right|^2$$

Using (15) and (9) one can obtain useful expression for the back scattering cross section of meteorological target:

$$\sigma = 4\pi \left| \hat{f}_b \right|^2 \quad \left[\text{m}^2 \right] \tag{16}$$

where \hat{f}_b is back scattering function, see (9).

5. Asymptotical Approaches of Back Scattering Cross Sections

For the asymptotical back scattering cross section computations it is convenient to work with the normalized cross sections σ_{NORM} [5], which is given as follows:

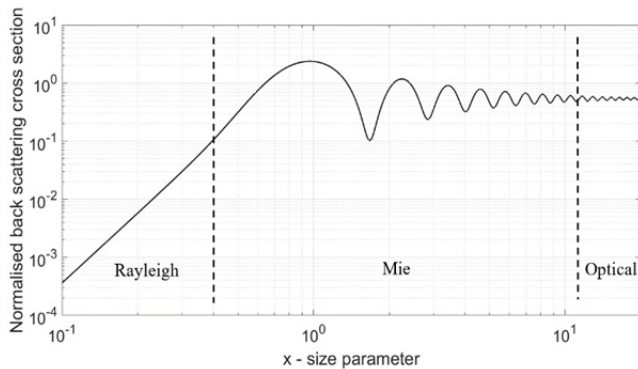


Fig. 3. Normalized back scattering cross section σ_{NORM} for 35 GHz and water drop target. Scattering regions (Rayleigh, Mie and optical ones) are labeled.

$$\sigma_{\text{NORM}} = \frac{\sigma}{\frac{1}{4} \cdot \pi \cdot D^2} \tag{17}$$

where D is the drop diameter.

It was found that σ_{NORM} as a function of size parameter x , is having two asymptotes: 1) in a so called optical region (in fact it is a geometrical optics zone, cf. [2]). 2) in so called Rayleigh region. We see them in Fig. 3 (similar results on higher frequencies were published in [2]). The central region with oscillations is usually called Mie region, in [2] it is called transition zone.

5.1 Approximation for Optical Region

Optical region is defined through the following inequalities:

$$x \gg 1 \text{ and } x_R \gg 1$$

whereas x (x_R) is so-called size parameter (size parameter in drop water) defined as

$$x = \pi D / \lambda, \tag{18}$$

$$x_R = \pi D / \lambda_R, \tag{19}$$

where λ is vacuum wave length and λ_R is wave length in the rain (cloud, fog) drop, i.e. in water. For wavelength λ_R in drop water it is valid:

$$\lambda_R = \lambda / |\hat{m}| \tag{20}$$

where \hat{m} is the complex refractive index of rain (cloud, fog) water, see, for instance [24], [25]. Size parameter is in fact the ratio of the circumference of the circle circumscribed around the drop to the wavelength.

Under such conditions ($x \gg 1$ and $x_R \gg 1$) in the optical region it is valid:

$$\sigma_{\text{NORM}} \approx L \text{ ("limit")} \tag{21}$$

where L is a constant dependent on frequency and temperature. We computed the limit values L and present these results in Fig. 4 as a function of frequency and for temperature of 15°C. May you remember that in case of metallic sphere it holds $L = 1$.

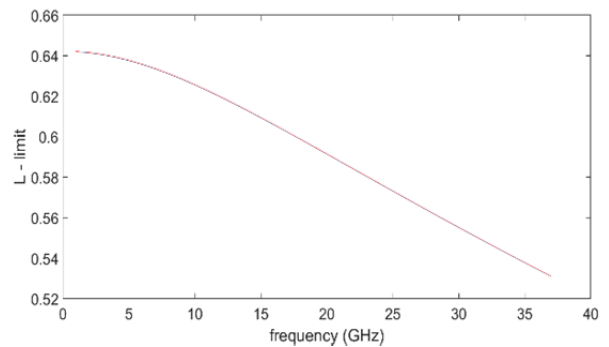


Fig. 4. L (limit) for normalized back scattering cross sections in optical region.

Practically this means that in the optical region the back scattering cross section equals to the circle area of the same radius like the spherical scattering multiplied by the constant L presented in Fig. 4. After our numerical investigations the condition $x \gg 1$ for optical region can be replaced by $x > x_{critO}$. Also for Rayleigh region (see the next section) we prefer the condition $x < x_{critR}$ to condition $x \ll 1$. These conditions are more unique and comfortable for definition of the optical and/or Rayleigh regions. This is one of our contributions to this topic.

In Tab. 1 “critical” values of x (x_{crit}) are shown for certain frequencies used in radar meteorology.

And how the values of x critical, i.e. x_{crit} , have been found? All the considerations given here are motivated by the effort to determine the drop back scattering cross section by a sufficient accuracy. We set a condition that the asymptotic value of the back scattering cross section cannot differ from the exact value by more than 1.26%. This corresponds approximately to a maximum estimation error of 1 dB for the radar reflectivity factor Z (26), (27).

The reader can find x critical values for the optical region in Fig. 5 and for the Rayleigh region in Fig. 6. Values of x critical for frequencies 29–35 GHz in Rayleigh region varies between 0.28 and 0.29 and are not plotted.

f [GHz]	Rayleigh region x_{critR}	Optical region x_{critO}
2.9	0.050	31.450
5.5	0.054	33.850
9.5	0.063	36.550
35	0.281	37.550

Tab. 1. Values of critical size parameter x_{crit} for Rayleigh and optical regions.

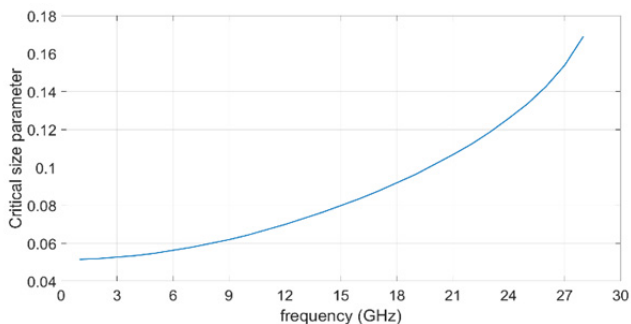


Fig. 5. Critical size parameter x_{critO} for optical region.

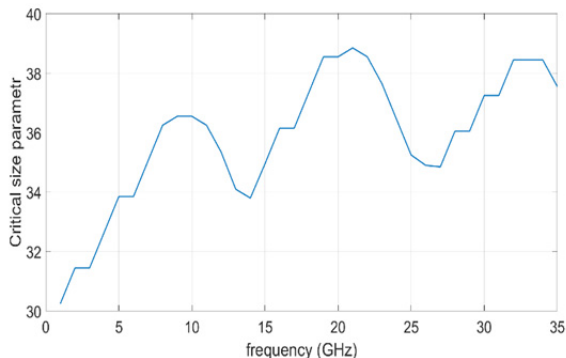


Fig. 6. Critical size parameter x_{critR} for Rayleigh region.

5.2 Rayleigh Approximation for Rayleigh Region

Rayleigh region is described by the following inequalities:

$$x \ll 1 \text{ and } x_R \ll 1.$$

For this region Mr. Strutt [26], [27] derived a simplified approximation for “the back scattering function” using elementary dipole theory:

$$\hat{f}_b \approx \frac{\pi^2 \cdot \hat{K}}{2\lambda^2} \cdot D^3 \tag{22}$$

where \hat{K} is an auxiliary parameter:

$$\hat{K} = \frac{\hat{m}^2 - 1}{\hat{m}^2 + 2}. \tag{23}$$

And then with the use of (16) the back scattering cross section σ in Rayleigh region is approximated by the next equation:

$$\sigma \approx \frac{\pi^5 |\hat{K}|^2}{\lambda^4} \cdot D^6. \tag{24}$$

For this work, Mr. Strutt received a noble title and the honor name “lord Rayleigh.”

The computation of the Rayleigh scattering is very simple (a handy calculator is sufficient) but we must be aware of strict limitations. We noticed that the frequency above about 5 GHz is owing to the usual rain drop diameter out of Rayleigh region.

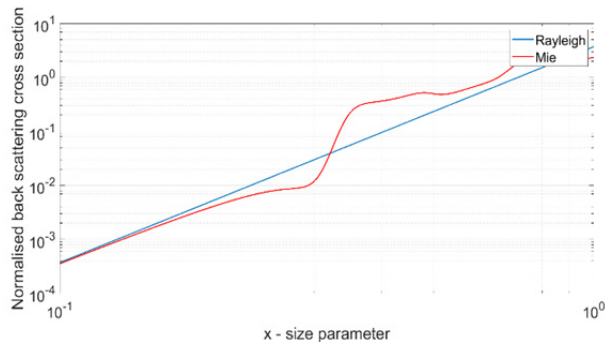


Fig. 7. Normalized back scattering cross sections for 2.9 GHz.

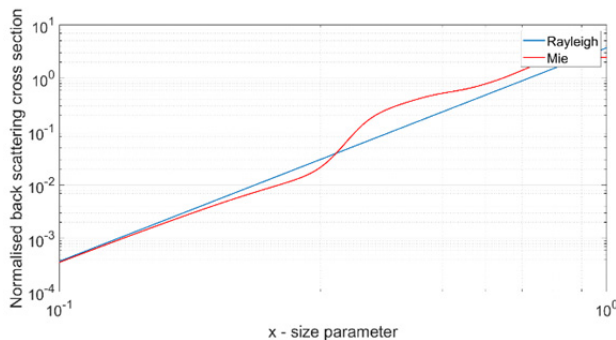


Fig. 8. Normalized back scattering cross sections for 5.5 GHz.

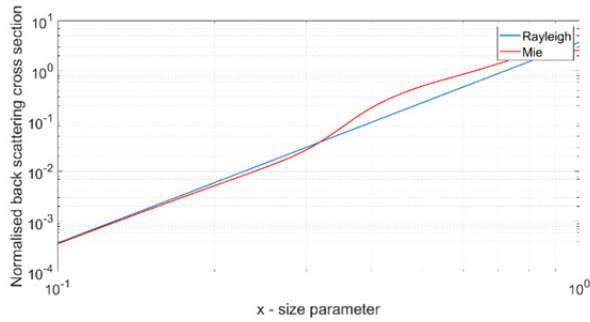


Fig. 9. Normalized back scattering cross sections for 9.5 GHz.

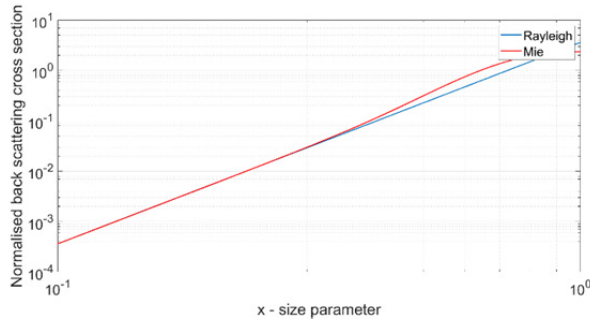


Fig. 10. Normalized back scattering cross sections for 35 GHz.

In log-log scale the dependence of σ_{NORM} on size parameter x looks like linear one because the relation (24) using (18) can be rewritten as:

$$\sigma_{\text{NORM}} \approx 4x^4 |\hat{\mathbf{K}}|^2. \quad (25)$$

In Figs. 7–10 the normalized back scattering cross sections for radar frequencies are shown. We consider the Mie solution to be the exact one.

Remark: Having a look at Figs. 7–10 one can notice that it seems the differences between normalized cross sections after Rayleigh and Mie are unlogically decreasing with frequency. We checked it – when we limit for $x < x_{\text{critR}}$ (Rayleigh region), this difference increases with frequency as expected.

Equation for scattering on homogenous ellipsoids in Rayleigh region is shown, for instance, in [7].

6. Radar Reflectivity Factor versus Equivalent Radar Reflectivity Factor

As it is shown in Sec. 2, meteorological radars measure the radar reflectivity η , cf. (2), (3) and (7). But this quantity is dependent on frequency. Therefore, in meteorology we work with the similar quantity called “radar reflectivity factor z ” being independent on frequency. The radar reflectivity z (small letter z) factor is defined [5] as

$$z = \int_0^{\infty} D^6 N(D) dD \quad [\text{mm}^6 \text{m}^{-3}]. \quad (26)$$

In practice in meteorology we work with the “dBZ” units as a unit for the radar reflectivity factor Z (in this case a capital letter “ Z ” is used) expressed in the logarithmic (or dB) form:

$$Z = 10 \cdot \log(z) \quad [\text{dBZ}]. \quad (27)$$

For Z expressed in [dBZ] the quantity “small” z in (27) must be in the $[\text{mm}^6 \text{m}^{-3}]$ units.

And now an important question: How to measure the radar reflectivity factor Z (or z)? We must state that it is not possible. But we can approximate the radar reflectivity factor through the “equivalent radar reflectivity factor z_e ” being less dependent on frequency:

$$z \approx z_e \quad (28)$$

while z_e is estimated from the next equations:

$$z_e \approx \frac{\lambda^4}{\pi^5 \cdot |\hat{\mathbf{K}}|^2} \cdot \eta \quad [\text{mm}^6 \text{m}^{-3}], \quad (29)$$

$$Z_e = 10 \cdot \log(z_e) \quad [\text{dBZ}] \quad (30)$$

while radar reflectivity η is measured through radar equation in meteorology (7).

This approximation is generally accepted. By our investigation we reached the conclusion that the expression for equivalent radar reflectivity factor Z_e (29), (30) approximates the wanted right radar reflectivity factor Z (26), (27) correctly only on low frequencies, it means in the Rayleigh region. Indeed, equation (29) comes from combination of (3) and (24), which is suggested and valid in

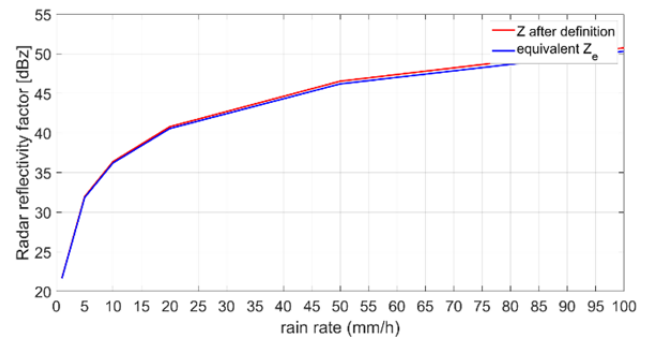


Fig. 11. Radar reflectivity factor for 2.9 GHz.

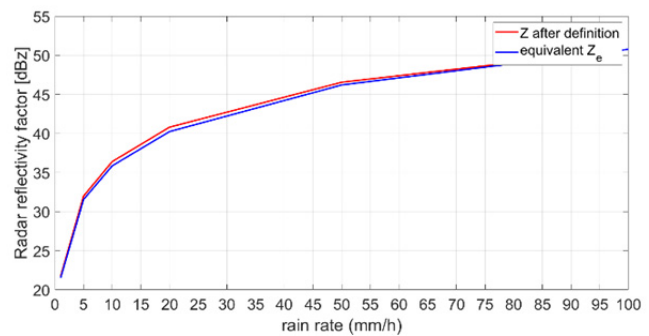


Fig. 12. Radar reflectivity factor for 5.5 GHz.

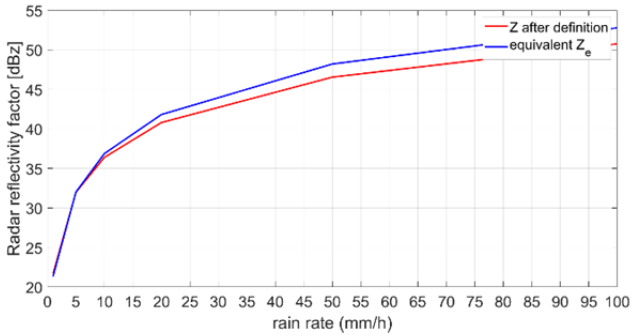


Fig. 13. Radar reflectivity factor for 9.5 GHz.

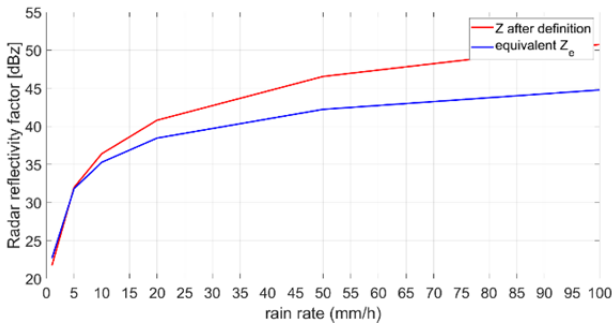


Fig. 14. Radar reflectivity factor for 35 GHz.

Rain type	N_0 [mm ⁻¹ m ⁻³]	λ_{DSD} [mm ⁻¹]
Thunderstorm or shower	1 400	$3.0 R^{-0.21}$
Continuous rain	7 000	$4.1 R^{-0.21}$
Drizzle	30 000	$5.7 R^{-0.21}$
Average rain	8 000	$4.1 R^{-0.21}$

Tab. 2. DSD parameters for negative exponential DSD approximation (31) and for various rain types (drizzle, thunderstorm, shower, continuous and average rain in mild climate after [8]. R is the rain rate [mm/h].

the Rayleigh region only. We proved that on higher frequencies the difference between radar reflectivity factor Z and equivalent one (Z_e) is not negligible. It can be noticed in Figs. 11–14. These differences between Z_e and Z on high frequencies led us to formulate the correction function (see the next section). To quantify expressions containing integral with DSD [i.e. $N(D)$ in (3) or (26)] we used the average Marshal-Palmer [8] mathematical model, where rain rate R is a parameter:

$$N(D) = N_0 \exp[-\lambda_{DSD}(R)D] \quad (31)$$

and $\lambda_{DSD}(R)$ is a parameter dependent on rain type and rain rate, see Tab. 2 taken from [9]. In our computation we used the average rain parameters after [8], see the last row in Tab. 2. R is the rain rate [mm/h].

7. Correction Function

We have stated the generally used radar reflectivity factor Z (26), (27) is not measurable by radar. Radar measures the radar reflectivity (3) and the wanted radar reflectivity factor Z is approximated by the equivalent radar

reflectivity factor Z_e through (29), (30) while radar reflectivity η is derived through radar measurement and radar equation in meteorology (7).

In previous sections we presented the mathematical apparatus enabling the theoretical computation of actual radar reflectivity factor. This enabled us to formulate the correction function C , which is in dB and is calculated as a difference of Z_e and Z (both are in dBZ), see (32). This correction function is designed for frequencies from 1 to 35 GHz and for rain rates 1, 5, 10, 20, 50 and 80 mm/h:

$$C = Z_e - Z \quad [\text{dB}]. \quad (32)$$

We approximated the suggested correction function C by a polynomial of the fifth degree (see also Tab. 3):

$$C \approx a_5 f^5 + a_4 f^4 + a_3 f^3 + a_2 f^2 + a_1 f + a_0 \quad [\text{dB}] \quad (33)$$

where f is frequency in GHz. Figures 15 and 16 show the graphs of the correction function C . Correction function is our other contribution on radar data analysis.

Rain rate [mm/h]	a_5	a_4	a_3	a_2	a_1	a_0
1	7.6850E-7	-6.098E-5	0.0013	-0.0014	-0.1102	0.2014
5	-8.8502E-7	0.0001	-0.0051	0.0990	-0.6386	0.8244
10	-2.0816E-6	0.0002	-0.0089	0.1483	-0.8335	0.9690
20	-3.1796E-6	0.0003	-0.0119	0.1814	-0.9011	0.9007
50	-4.1468E-6	0.0004	0.0140	0.1905	0.7703	0.4903
80	-4.4178E-6	0.0004	0.0142	0.1828	0.6349	0.1941

Tab. 3. Coefficients for polynomial approximation of the correction function C in [dB] for frequencies between 1–35 GHz while rain rate R is a parameter.

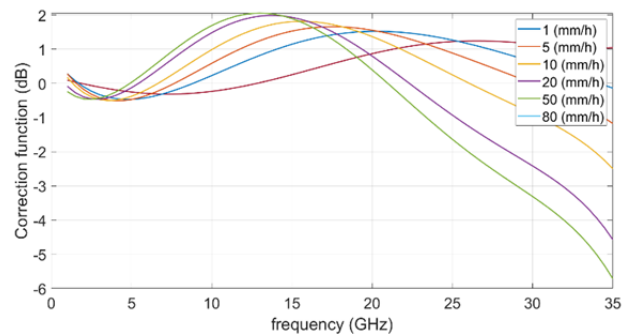


Fig. 15. Correction function (32), R is rain rate [mm/h].

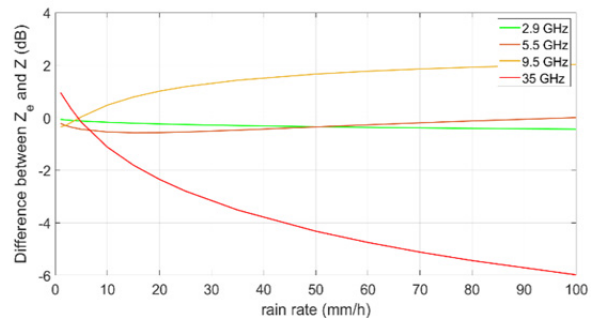


Fig. 16. Differences between equivalent radar reflectivity factor Z_e and radar reflectivity factor Z for different frequencies (correction function C).

8. Conclusion

Finally, let's try to emphasize what this article should be for. It should help propagation engineers to understand what a meteorological radar is actually measuring.

Meteorological radar can also estimate the rain rate R , for these purposes we derived the next equation:

$$R = 10^{\left(\frac{Z}{16}\right)^{1.44}} \text{ [mm/h, dBZ]} \tag{34}$$

which is based on well-known approximate Z-R relation for average rain type:

$$Z = 10 \log(200 R^{1.6}) \text{ [dBZ, mm/h].} \tag{35}$$

Knowing rain rate R from radar measurement (34), specific rain attenuation α (important for microwave link design) can be then estimated from the equation

$$\alpha = a \cdot R^b \text{ [dB/km, mm/h]} \tag{36}$$

where a and b are parameters dependent on frequency, polarization and elevation angle of the microwave link and are tabulated, for instance, in [28].

Let us now consider regions in which specific raindrops or fog (cloud) droplets are located for often frequencies used in radar meteorology. For these reasons we prepared Tab. 4 where we see the equivolumetric diameters D of the rain drops in the left column, in the fields of the table there is the size parameter x (18) for different radar frequencies. From the comparison with x critical, we marked the drops in the Rayleigh region in blue. Other drops are in the Mie region, no raindrop is in the optical region. We prepared a similar table for the usual sizes of fog (cloud) droplets, whose diameter is between 2 and 80 micrometers. For the meteorological radar frequencies (2.9–35 GHz) we found all these droplets in the Rayleigh region and therefore the table does not need to be given.

Wavelength [cm]	10.34	5.45	3.15	0.86
Frequency [GHz]	2.9	5.5	9.5	35
D[mm] = 0.22	0.01	0.01	0.02	0.08
0.42	0.01	0.02	0.04	0.15
0.62	0.02	0.04	0.06	0.23
0.82	0.02	0.05	0.08	0.30
1.02	0.03	0.06	0.10	0.37
1.22	0.04	0.07	0.12	0.45
1.42	0.04	0.08	0.14	0.52
1.62	0.05	0.09	0.16	0.59
1.82	0.06	0.10	0.18	0.67
2.02	0.06	0.12	0.20	0.74
...				
7.00	0.21	0.39	0.68	2.50

Tab. 4. Classification of raindrops into regions, blue for Rayleigh region, gray for Mie region. The values in table are size parameters x .

The next remark concerns the reality of the existence of droplets corresponding to size parameter x and the considered radar frequency. It should be noted that some x values at a given radar frequency do not correspond to the diameters of the droplets existing in nature. For instance raindrops have a diameter from 0.2 to 7 mm in nature. However, some value of x in our considerations corresponds to D greater than 7 mm - it must be declared that such a drop does not exist and our analysis is of theoretical importance in such cases.

The last remark: We presented the approximations for normalized back scattering cross sections for both Rayleigh and optical region. Approximation for Mie region is more complicated because of oscillations (see Fig. 3) and can be found (and much more) in [5].

Acknowledgments

This study was thankfully supported from the ERDF/ESF "Cooperation in Applied Research between the University of Pardubice and companies, in the Field of Positioning, Detection and Simulation Technology for Transport Systems (PosiTrans)" project (No. CZ.02.1.01/0.0/0.0/17_049/0008394).

References

- [1] HUUSKONEN, A., SALTIKOFF, E., HOLLEMAN, I. The operational weather radar network in Europe. *Bulletin of the American Meteorological Society*, 2014, vol. 95, no. 6, p. 897–907. DOI: 10.1175/BAMS-D-12-00216.1
- [2] SASSEN, K., CAMPBELL, J. R., ZHU, J., et al. Lidar and triple-wavelength Doppler radar measurements of the melting layer: A revised model for dark- and brightband Phenomena. *Journal of Applied Meteorology*, 2005, vol. 44, no. 3, p. 301–312. DOI: 10.1175/JAM-2197.1
- [3] LAMER, K., OUE, M., BATTAGLIA, A., et al. Multifrequency radar observations of clouds and precipitation including the G-band. *Atmospheric Measurement Techniques*, 2021, vol. 14, no. 5, p. 3615–3629. DOI: 10.5194/amt-14-3615-2021
- [4] KNIGHT, C. A., MILLER, L. J. First radar echoes from cumulus clouds. *Bulletin of the American Meteorological Society*, 1993, vol. 74, no. 2, p. 179–188.
- [5] ATLAS, D. (Ed.) *Radar in Meteorology*. Springer, 1990. ISBN: 978-1-935704-15-7 DOI: 10.1007/978-1-935704-15-7
- [6] D'AMICO, M. *An Anisotropic Model of the Electromagnetic Properties of the Melting Layer, and Comparison with Radar Observations*. Ph.D. Thesis. University of Essex (UK), 1997.
- [7] TRIDON, F., BATTAGLIA, A., Dual-frequency radar Doppler spectral retrieval of rain drop size distributions and entangled dynamics variables: Radar Doppler spectral retrieval in rain. *Journal of Geophysical Research: Atmospheres*, 2015, vol. 120, no. 11, p. 5585–5601. DOI: 10.1002/2014JD023023
- [8] MARSHALL, J. S., PALMER, W. M. The distribution of raindrops with size. *Journal of Meteorology*, 1948, vol. 5, no. 4, p. 165–166. DOI: 10.1175/1520-0469(1948)005<0165:TDORWS>2.0.CO;2

- [9] JOSS, J., THAMS, J. C., WALDVOGEL, A. The Variation of Raindrop Size Distributions at Locarno. *ETH: Wissenschaftliche Mitteilungen / Eidgenössische Kommission zum Studium der Hagelbildung und der Hagelabwehr*. 1970, p. 1–7.
- [10] MORRISON, J. A., CROSS, M. J., Scattering of a plane electromagnetic wave by axisymmetric raindrops. *Bell System Technical Journal*, 1974, vol. 53, no. 6, p. 955–1019. DOI: 10.1002/j.1538-7305.1974.tb02779.x
- [11] UZUNOGLU, N. K., EVANS, B. G., HOLT, A. R. Scattering of electromagnetic radiation by precipitation particles and propagation characteristics of terrestrial and space communication systems. In *Proceedings of the Institution of Electrical Engineers*, 1977, vol. 124, no. 5, p. 417–424. DOI: 10.1049/ptee.1977.0078
- [12] FISER, O. A simple generator of forward scattering functions on spherical dielectrics. *Radioengineering*, 1993, vol. 2, no. 1, p. 21–22. ISSN: 1210-2512
- [13] MIE, G. Contributions to the optics of turbid media, especially colloidal metal solutions (Beiträge zur Optik trüber Medien, speziell kolloidaler Metallösungen). *Annalen der Physik*, 1908, vol. 25, no. 3, p. 377–445. (In German) DOI: 10.1002/andp.19083300302
- [14] MISHCHENKO, I. M., Gustav Mie and the fundamental concept of electromagnetic scattering by particles: A perspective. *Journal of Quantitative Spectroscopy and Radiative Transfer*. 2009, vol. 110, no. 14–16, p. 1210–1222. DOI: 10.1016/j.jqsrt.2009.02.002
- [15] MÄTZLER, C. MATLAB functions for Mie scattering and absorption, version 2. *Technical Report*, 2002, IAP Res. Rep., University of Bern.
- [16] COX, A. J., DE WEERD, A. J., LINDEN, J. An experiment to measure Mie and Rayleigh total scattering cross sections. *American Journal of Physics*, 2002, vol. 70, no. 6, p. 620–625. DOI: 10.1119/1.1466815
- [17] PRUPPACHER, H. R., PITZER, R. L. A semi-empirical determination of the shape of clouds and raindrops. *Journal of the Atmospheric Sciences*, 1971, vol. 28, no. 1, p. 86–94. DOI: 10.1175/1520-0469(1971)028<0086:ASEDOT>2.0.CO;2
- [18] OGUCHI, T. Scattering properties of oblate raindrops and cross polarization of radio waves due to rain: Calculations at 19.3 and 34.8 GHz. *Journal of Radio Research Laboratories*, 1973, vol. 20, no. 102, p. 79–119.
- [19] OGUCHI, T. Electromagnetic wave propagation and scattering in rain and other hydrometeors. In *Proceedings of the IEEE*, 1983, vol. 71, no. 9, p. 1029–1078. DOI: 10.1109/PROC.1983.12724
- [20] HAJNY, M., MAZANEK, M., FISER, O. Ku-band rain scattering parameters calculated by MMP method. In *Proceedings of the First International Workshop on Radiowave Propagation Modelling for SatCom Services at Ku band and above*. Noordwijk (The Netherlands), 1998.
- [21] MAGGIORI, D. Computed transmission through rain in the 1–400 GHz frequency range for spherical and elliptical drops and any polarization. *Alta Frequenza*, 1981, vol. 50, no. 5, p. 262–273.
- [22] LEVIZZANI, V., KIDD, CH., KIRSCHBAUM, D. B., et al. (Eds.) *Satellite, Precipitation Measurement*. (Vol. 1, chapter 15) Springer, 2020. ISBN: 978-3-030-24568-9
- [23] ERIKSSON, P., EKELUND, R., MENDROK, J., et al. A general database of hydrometeor single scattering properties at microwave and sub-millimetre wavelengths. *Earth System Science Data*, 2018, vol. 10, no. 3, p. 1301–1326. DOI: 10.5194/essd-10-1301-2018
- [24] RAY, P. Broadband complex refractive indices of ice and water. *Applied Optics*, 1972, vol. 11, no. 8, p. 1836–1844. DOI: 10.1364/AO.11.001836
- [25] LIEBE, H. J. MPM - An atmospheric millimeter-wave propagation model. *International Journal of Infrared and Millimeter Waves*, 1989, vol. 10, p. 631–650. DOI: 10.1007/BF01009565
- [26] STRUTT, J. W. On the light from the sky, its polarization and colour (I). *Philosophical Magazine*, 1871, Series 4, vol. 41, no. 271, p. 107–120. DOI: 10.1080/14786447108640452
- [27] STRUTT, J. W. On the light from the sky, its polarization and colour (II). *Philosophical Magazine*, 1871, Series 4, vol. 41, no. 273, p. 274–279. DOI: 10.1080/14786447108640479
- [28] INTERNATIONAL TELECOMMUNICATION UNION (ITU). *Recommendation ITU-R P.838-3, Specific Attenuation Model for Rain for Use in Prediction Methods*. Question ITU-R 201. 2013
- [29] BOHREN, C. F., HUFFMAN, D. R. *Absorption and Scattering of Light by Small Particles*. New York (USA): John Wiley, 1983. ISBN: 9780471293408
- [30] MATROSOV, S. Y. Evaluating polarimetric X-band radar rainfall estimators during HMT. *Journal of Atmospheric and Oceanic Technology*, 2010, vol. 27, no. 1, p. 122–134. DOI: 10.1175/2009JTECHA1318.1

About the Authors ...

Ondřej FIŠER (corresponding author) was born in Prague, Czech Republic in 1952. He received his Master's degree in Electro-Engineering (field: Theory of Electromagnetic Field, 1977) and Ph.D. title (field: Radio-Wave Propagation, 1986), both from the Electrotechnical Faculty, Czech Technical University in Prague. All his professional life he has worked in the field of radiowave or optical wave propagation research and radar meteorology. He has started at the TESTCOM, previously Telecommunication Research Institute (1978–1993). From 1993 on, he has worked as a scientist researcher at the Institute of Atmospheric Physics of the Czech Academy of Sciences in Prague. Since 2003 he has also taught the High Frequency Technology and Electromagnetic Compatibility at the Faculty of Electrical Engineering and Informatics of the University of Pardubice (in the town of Pardubice, CZ), as an Associated Professor. He was acting within many international research projects, like INTERKOSMOS, OPEX, RADHYD, PADRE, COST, ESA projects etc. Dr. Fiser became a Member of IEEE in 2018 and is a member of the Czech National URSI committee since 1999. He is the author of dozens of articles, contributions and book chapters based on his research.

Maria KOVALCHUK was born in Pervouralsk, Russia, in 1993. She received the B.S. degrees in Information Technology and Communication Systems from the Ural Technical Institute of Communications and Informatics, Yekaterinburg, Russia, in 2016 and M.S. degrees in Electrical Engineering and Informatics from the University of Pardubice, CZ, in 2019. Now she is currently pursuing the Ph.D. degrees in Electrical Engineering from the University of Pardubice, Pardubice, CZ. Since 2019 she has been a scientist researcher in meteorological field at the Institute of Atmospheric Physics AS CR, Prague. She is focusing on radio wave propagation in troposphere, radar meteorology and EMC.